JOURNAL OF VIROLOGY, Nov. 2011, p. 11079–11089 Vol. 85, No. 21
0022-538X/11/$12.00 doi:10.1128/JVI.05098-11

Varicella-Zoster Virus Immediate-Early Protein ORF61 Abrogates the IRF3-Mediated Innate Immune Response through Degradation of Activated IRF3[▽]

Huifang Zhu,[1]# Chunfu Zheng,[1]#* Junji Xing,[1] Shuai Wang,[1] Shuping Li,[2] Rongtuan Lin,[3] and Karen L. Mossman[4]

Molecular Virology and Viral Immunology Research Group, State Key Laboratory of Virology, Wuhan Institute of Virology, Chinese Academy of Sciences, Wuhan 430071, China[1]; State Key Laboratory for Diagnosis and Treatment of Infectious Diseases, The First Affiliated Hospital, School of Medicine, Zhejiang University and Key Laboratory of Infectious Diseases, Zhejiang 310058, China[2]; The Terry Fox Molecular Oncology Group, Lady Davis Institute for Medical Research, Department of Medicine, McGill University, Montreal, Quebec H3T 1E2, Canada[3]; and Department of Pathology and Molecular Medicine, Institute for Infectious Disease Research, McMaster University, Hamilton, Ontario L8N 3Z5, Canada[4]

Received 12 May 2011/Accepted 22 July 2011

Varicella-zoster virus (VZV) infection of differentiated cells within the host and establishment of latency likely requires evasion of innate immunity and limits secretion of antiviral cytokines. Here we report that its immediate-early protein ORF61 antagonizes the beta interferon (IFN-β) pathway. VZV infection down-modulated the Sendai virus (SeV)-activated IFN-β pathway, including mRNA of IFN-β and its downstream interferon-stimulated genes (ISGs), ISG54 and ISG56. Through a primary screening of VZV genes, we found that ORF61 inhibited SeV-mediated activation of IFN-β and ISRE (IFN-stimulated response element) promoter activities but only slightly affected NF-κB promoter activity, implying that the IFN-β pathway may be blocked in the IRF3 branch. An indirect immunofluorescence assay demonstrated that ectopic expression of ORF61 abrogated the detection of IRF3 in SeV-infected cells; however, it did not affect endogenous dormant IRF3 in noninfected cells. Additionally, ORF61 was shown to be partially colocalized with activated IRF3 in the nucleus upon treatment with MG132, an inhibitor of proteasomes, and the direct interaction between ORF61 and activated IRF3 was confirmed by a coimmunoprecipitation assay. Furthermore, Western blot analysis demonstrated that activated IRF3 was ubiquitinated in the presence of ORF61, suggesting that ORF61 degraded phosphorylated IRF3 via a ubiquitin-proteasome pathway. Semiquantitative reverse transcription-PCR (RT-PCR) analysis demonstrated that the level of ISG54 and ISG56 mRNAs was also downregulated by ORF61. Taken together, our results convincingly demonstrate that ORF61 down-modulates the IRF3-mediated IFN-β pathway by degradation of activated IRF3 via direct interaction, which may contribute to the pathogenesis of VZV infection.

Varicella-zoster virus (VZV) is ubiquitous in most of the population worldwide and is an alphaherpesvirus restricted to humans. Primary VZV infection begins with inoculation of the respiratory mucosa, followed by cell-associated viremia and the rash of chickenpox. During primary infection, the virus establishes latency in sensory ganglia and can subsequently reactivate to cause shingles (herpes zoster) (3). The VZV genome contains one copy of linear double-strand DNA approximately 125 kb in length and encodes about 70 unique proteins. Similar to other alphaherpesviruses, the expression of VZV genes is assorted temporally into three categories—immediate-early (IE), early (E), and late (L)—and the IE proteins usually play critical roles during VZV life cycles (29).

ORF61 encodes a 62- to 66-kDa phosphoprotein (45), which is highly homologous to herpes simplex virus 1 (HSV-1) ICP0 in the RING finger domain and can partially complement the function of ICP0 in ICP0-null HSV-1 (28). Both proteins exhibit regulatory functions, but the difference between them is that ORF61 has either a transactivated or repressive function (16, 31), while ICP0 mostly shows transcriptional activation (12, 14). Although ICP0 can inhibit the innate immunity pathway at many levels, such as IRF3 and PML (13, 26), little is known about the function of ORF61 in interrupting the innate immunity.

The innate immune system is an ancient and nonspecific system that provides the first line of defense against infection. One of the most effective innate antiviral responses is the production of alpha/beta interferon (IFN-α/β) and the subsequent induction of interferon-stimulated genes (ISGs) (38). Previous studies have demonstrated that VZV infection stimulates innate immune responses mainly by the production of IFN-α and IFN-γ (1, 2, 27), while IFN-β is not detected in serum of VZV-infected patients. This might be explained by the evidence provided by one group that the production of IFN-β may be blocked by ORF62 during VZV infection (40).

Increasing evidence has shown that ICP0 possesses various antagonistic functions against the host innate immune system

* Corresponding author. Mailing address: Wuhan Institute of Virology, Chinese Academy of Sciences, 44 Xiaohongshan Wuchang, Wuhan 430071 China. Phone and fax: 86-27-8719-8676. E-mail: zheng.alan@hotmail.com.
# These two authors contributed equally to the work.
▽ Published ahead of print on 10 August 2011.

(33); however, little is known about the function of ORF61 in interrupting innate immunity, especially in the IFN-β pathway. In the present study, we tried to determine the molecular mechanism by which ORF61 blocks the IFN-dependent antiviral response. We found that VZV infection could downmodulate the Sendai virus (SeV)-activated IFN-β pathway, and further study indicated that ORF61 inhibits SeV-mediated activation of IFN-β promoter activity in HEK 293T cells. ORF61 specifically blocks the IRF3-mediated innate immune responses, and its RING finger is critical for this activity. Interestingly, ORF61 targets only activated IRF3 for proteasome-mediated degradation by direct interaction. Two ISGs downstream of IFN-β, ISG54 and ISG56, were sharply downregulated in response to SeV stimulation in the presence of ORF61. These results expand our knowledge of both cellular antiviral responses to virus infection and the countermeasures adopted by VZV to ensure its successful replication and spread.

(The abstract of this paper was presented at the Institute Pasteur International Network Annual Scientific Meeting, 2010 [58]).

MATERIALS AND METHODS

Cells culture, virus infection, and reagents. HEK 293T cells and MeWo cells were grown in Dulbecco's modified minimum essential medium (DMEM; Gibco-BRL) supplemented with 10% fetal bovine serum (FBS) and 100 U/ml of penicillin and streptomycin. HeLa cells were maintained in Eagle's minimum essential medium (Gibco-BRL) supplemented with 10% fetal calf serum (FCS).

The pOka strain VZV (wild type [wt]) and VZV-GFP viruses, gifts from Hua Zhu (55), were grown in the human melanoma cell line MeWo. HEK 293T cells were infected with VZV by coculture with VZV-infected MeWo cells at a 1:1 ratio for 1 h at 37°C. Then the inoculum was removed with fresh DMEM, and HEK 293T cells were cultured in fresh medium.

The proteasome inhibitor MG132 was purchased from Sigma (St. Louis, MO). Rabbit antisera against IRF3(S396) were described previously (10); the protease inhibitor mixture cocktail and anti-Flag monoclonal antibody (MAb) were purchased from CST (Boston, MA). Rabbit anti-IRF3 polyclonal antibody (PAb) and anti-β-actin MAb were purchased from Proteintech (Wuhan, China). A rabbit anti-enhanced yellow fluorescent protein (EYFP) PAb was purchased from Santa Cruz Biotechnology, Inc. (Santa Cruz, CA).

Plasmid construction. All enzymes used for cloning procedures were purchased from Takara (Dalian, China) except T4 DNA ligase, which was obtained from New England BioLabs (Beverly, MA). To construct ORF61-Flag, the ORF61 gene was amplified from a VZV bacterial artificial chromosome (BAC) (Oka strain) and cloned into the EcoRI and BamHI sites of the pCMV-Flag vector (Beyotime, Shanghai, China) and the pEYFP-N1 vector (Clontech). A point mutation (C19G) was introduced into ORF61-Flag to disrupt the RING finger domain. *Homo sapiens* IRF3 was amplified from plasmid IRF3-GFP (21) and cloned into the EcoRI and KpnI sites of the pCMV-Flag vector (Beyotime) and the pEYFP-N1 vector (Clontech). Commercial reporter plasmids were NF-κB-luc (Stratagene, La Jolla, CA) and pRL-TK plasmid (Promega). Plasmids acquired as gifts included (PRDIII-I)4-Luc (11), ISRE (IFN-stimulated response element)-luciferase reporter plasmid (24), pcDNA3.1-FlagTBK1 (36), pcDNA3.1/Zeo-MAVS (36), pcDNA3.1-FlagIKKi (56), the IRF3-GFP plasmid (21), pEF-FlagRIG-IN (52), the IRF3/5D plasmid (7), the IRF7(6D) plasmid, a ubiquitin-hemagglutinin (HA) plasmid (36), pCAGGS-NS1 (19), and an IFN-β promoter reporter plasmid (22).

RNA isolation and semiquantitative RT-PCR. Total RNA was extracted from HEK 293T cells with TRIzol (catalog no. 15596-018; Invitrogen) according to the manufacturer's manual. Samples were digested with DNase I and subjected to reverse transcription-PCR (RT-PCR). RNA was reverse transcribed using an oligo(dT) primer. A mock reaction was carried out with no reverse transcriptase added. Ten percent of the resulting cDNA was used as a template for PCR using specific primers for human ISG54 and ISG56. The GAPDH (glyceraldehyde-3-phosphate dehydrogenase) gene was used as a housekeeping gene to establish a baseline against which target genes were compared between samples. Primer sequences were as follows: 5′-GACACCCACTCCTCCACCTTT-3′ (forward) and 5′-ACCACCCTGTTGCTGTAGCC-3′ (reverse) for hGAPDH, 5′-CAAATTGCTCTCCTGTTGTGCTTC-3′ (forward) and 5′-AATGCGGCGTCCTCCTTCT-3′ (reverse) for hIFN-β, 5′-ACGCATTTGAGGTCATCAGGGTG-3′ (forward) and 5′-CCAGTCGAGGTTATTTGGATTTGGTT-3′ (reverse) for hISG54, 5′-GCTTTCAAATCCCTTCCGCTAT-3′ (forward) and 5′-CTTGGCCCGTTCATAATTCTTTC-3′ (reverse) for hISG56. PCR products were analyzed on a 2% agarose gel.

Transfection and dual luciferase reporter (DLR) assay. The HEK 293T cells were plated onto 24-well dishes (Corning, NY) in DMEM (Gibco-BRL) with 10% FBS at a density about 1×10^5 cells per well overnight before transfection. Cells were then cotransfected with 500 ng of a reporter plasmid such as p125-luc or pISRE-luc and 2 μg of expression plasmid as indicated by standard calcium phosphate precipitation (17, 57). To normalize transfection efficiency, 50 ng of the *Renilla* luciferase reporter plasmid pRL-TK was added to each transfection. At 24 h posttransfection, cells were infected with SeV for 16 h, and luciferase assays were performed with a dual-specificity luciferase assay kit (Promega, Madison, WI). All reporter assays were carried out at least three times, and the results shown are averages and standard deviations from one representative experiment.

Immunofluorescence assay. Immunofluorescence assays were performed as described in our previous study (51). In brief, HeLa cells were observed either live or fixed in 4% paraformaldehyde in phosphate-buffered saline (PBS; 0.137 M NaCl, 0.003 M KCl, 0.008 M Na_2HPO_4, 0.001 M NaH_2PO_4 [pH 7.4]) for 20 min, washed three times with PBS, and permeabilized with 0.5% Triton X-100 in PBS for 10 min. The cells were rinsed with PBS and then incubated with PBS containing 5% bovine serum albumin (BSA) for 20 min at room temperature. Subsequently, the cells were incubated with IRF3-specific polyclonal rabbit antibody diluted in PBS containing 0.5% BSA for 2 h at 37°C, followed by incubation with fluorescein isothiocyanate (FITC)-conjugated goat anti-rabbit IgG (Sigma-Aldrich) in PBS containing 0.5% BSA for 1 h at 37°C. After each incubation step, cells were washed extensively with PBS. Samples were analyzed with a fluorescence microscope (Zeiss, Germany). Images were processed using Adobe Photoshop.

Coimmunoprecipitation assay. The coimmunoprecipitation (co-IP) assay was performed as described in our previous study (50). In brief, at 24 h posttransfection, HEK 293T cells were washed twice with phosphate-buffered saline and scraped in 500 to 800 μl of modified RIPA buffer [50 mM Tris-HCl (pH 7.4), 1% NP-40, 0.5% Na-deoxycholate, 0.15 M NaCl, 1 mM EDTA] or in lysis buffer [20 mM Tris-HCl, 150 mM NaCl, 1% NP-40] and a protease inhibitor mixture cocktail from CST (Boston, MA). After sonication, the supernatant was centrifuged at maximum speed on a tabletop centrifuge at 4°C for 15 min. Supernatants were collected and incubated with anti-Flag MAb or nonspecific control mouse antibody (IgG) and protein G agarose beads (CST, Boston, MA) overnight at 4°C with agitation. The mixture was washed three times with RIPA buffer, once with 150 mM NaCl, and three times in PBS, and then the samples were subjected to sodium dodecyl sulfate-polyacrylamide gel electrophoresis (SDS-PAGE) and Western blot analysis.

Western blot analysis. Western blot analysis was performed as previously described (35). Briefly, after transfection or SeV infection, whole-cell extracts were subjected to 10% SDS-PAGE and transferred to nitrocellulose membranes, followed by blocking with 5% nonfat milk in Tris-buffered saline–Tween (TBST; 50 mM Tris-HCl, 200 mM NaCl, 0.1% [vol/vol] Tween 20 [pH 7.5]), and probed with corresponding primary antibodies at 37°C for 2 h. After being washed with TBST, the membranes were incubated with alkaline phosphatase-conjugated goat anti-rabbit IgG or goat anti-mouse IgG (1:10,000 dilution) at 37°C for 1 h. Protein bands specific to the antibody were developed with 5-bromo-4-chloro-3-indolylphosphate (BCIP)–nitroblue tetrazolium (NBT), and the process was terminated by distilled water.

RESULTS

VZV infection inhibits the IRF3-mediated IFN-β pathway. To establish infections, viruses must subvert the antiviral response, which is mounted mainly by the cellular interferon system. A previous report demonstrated that VZV is extremely sensitive to type I and type II IFNs (4), which indicates that VZV needs to block the production of type I IFN during early infection to establish successful infection. To determine whether VZV infection could suppress the IFN-β pathway, DLR assays were performed to measure whether VZV infection affected

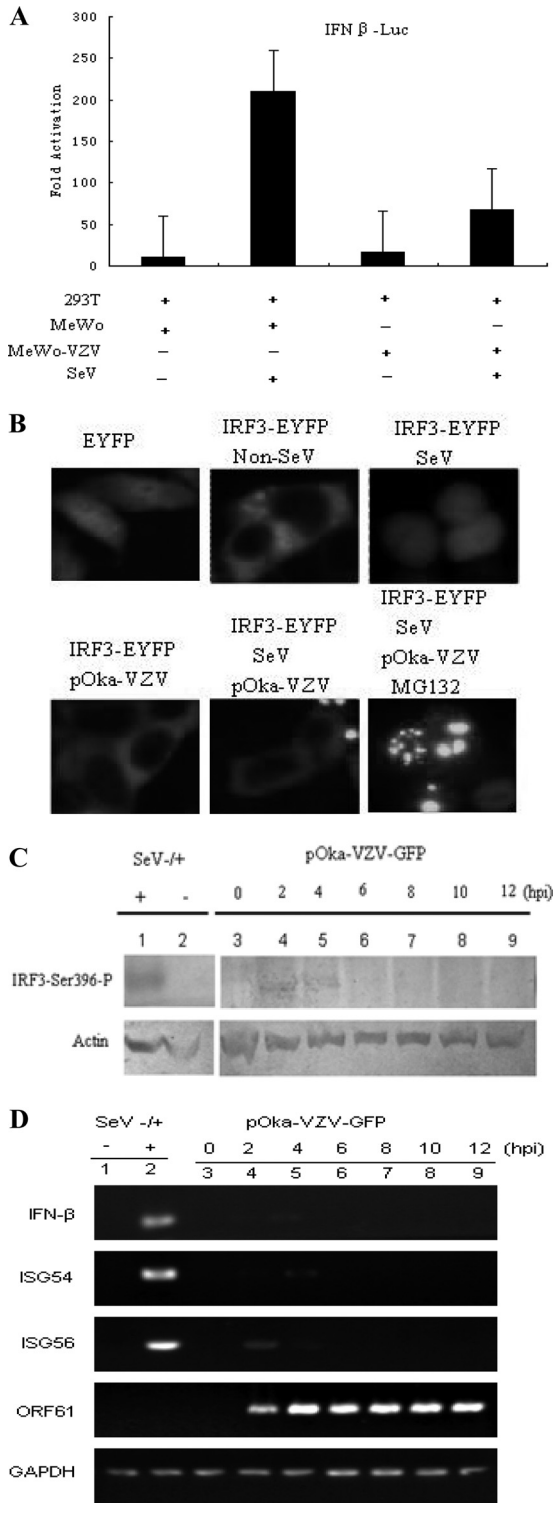

FIG. 1. VZV infection down-modulates the IRF3-mediated IFN-β pathway. (A) VZV infection inhibits SeV-activated IFN-β promoter activity. HEK 293T cells were cotransfected with the IFN-β reporter plasmid p125-luc and the *Renilla* luciferase plasmid pRL-TK. Twenty-four hours after transfection, HEK 293T cells were infected with 100 hemagglutinating units (HAU)/ml SeV or left uninfected, as indicated; at 8 hpi, VZV-infected MeWo cells were added to the pretreated HEK 293T cells at a ratio of 1 to 1 for 1 h at 37°C. Then the inoculum was removed with fresh DMEM, and HEK 293T cells were cultured in fresh medium for another 12 h until the luciferase activity was measured. Data are expressed as means and standard deviations from three independent experiments performed in duplicate. (B) MeWo cells were transfected with pEYFP or IRF3-EYFP; 24 h after transfection, cells were treated with 100 HAU/ml SeV or left uninfected. At 8 hpi, VZV-infected MeWo cells were added to the pretreated MeWo cells at a ratio of 1 to 1 for 1 h at 37°C. Then the inocula were removed with fresh DMEM, and the infected cells were cultured in fresh medium for another 12 h before fluorescence microscopy analysis. (C) Activated IRF3 during VZV infection. HEK 293T cells were seeded onto 35-mm cell culture plates; after 24 h, VZV-infected MeWo cells were added to the cells at a ratio of 1 to 1 for 1 h at 37°C. Then the inoculum was removed with fresh DMEM, and HEK 293T cells were cultured in fresh medium. Whole-cell extracts were collected at the indicated time points for Western blot analysis of IRF3-Ser396. (D) VZV infection downregulates the levels of mRNAs of IFN-β and downstream ISGs. HEK 293T cells were infected with VZV as described for panel B. Total RNA was extracted at the indicated time points for semiquantitative RT-PCR analysis.

the IFN-β promoter activity stimulated by SeV. VZV infection inhibited SeV-mediated IFN-β promoter activity about 4-fold (Fig. 1A). This is a crucial finding in the investigation of the relationship between VZV infection and the host innate immune response. Furthermore, semiquantitative RT-PCR was performed to detect the mRNA level of IFN-β and downstream ISGs, ISG54 and ISG56, during VZV early infection. As expected, IFN-β transcripts could not be detected during VZV infection between 2 and 12 hours postinfection (hpi); this indicates that neither ISG54 nor ISG56 mRNA was upregulated upon VZV infection (Fig. 1D). It is well known that SeV is a practicable model virus to evoke the host innate immune response via the RIG-I/MDA5-IRF3-IFN-β pathway whose infection is usually used as a positive control. The IFN-β mRNA level was highly upregulated in SeV-infected cells compared to noninfected cells, as well as the ISG54 and ISG56 mRNA levels (Fig. 1D). IRF3 is one of the most important cellular transcription factors and plays a central role in the IFN-β pathway. In resting cells, IRF3 usually localizes in the cytoplasm, and in response to virus infection, IRF3 experiences a sequential change: it is first phosphorylated by two kinases, TBK1 and IKKi; next it undergoes dimer formation; and last, it translocates into the nucleus as an activated transcription factor. Accordingly, the subcellular localization of IRF3 was investigated to determine the effect of VZV infection on the IRF3-IFN-β signaling pathway. IRF3-EYFP localized in the cytoplasm in resting MeWo cells, and it translocated to the nucleus upon SeV infection (Fig. 1B). However, IRF3-EYFP in VZV-infected cells remained in the cytoplasm during SeV infection (Fig. 1B), suggesting that VZV infection abrogated the translocation of IRF3 from the cytoplasm to the nucleus in the IFN-β signaling pathway. Usually, the phosphorylation of IRF3-Ser396 is a typical response to virus infection. Western blot (WB) analysis showed that phosphorylated IRF3 on Ser396 was detectable during VZV early infection between 2 and 4 hpi with phosphospecific IRF3(S396) antibody; however, no phosphorylated IRF3 was detected thereafter (Fig. 1C). These results demonstrate that the IRF3-mediated IFN-β pathway was blocked during VZV infection.

ORF61 inhibits SeV-mediated activation of IFN-β promoter activity. During VZV infection, the innate immunity response

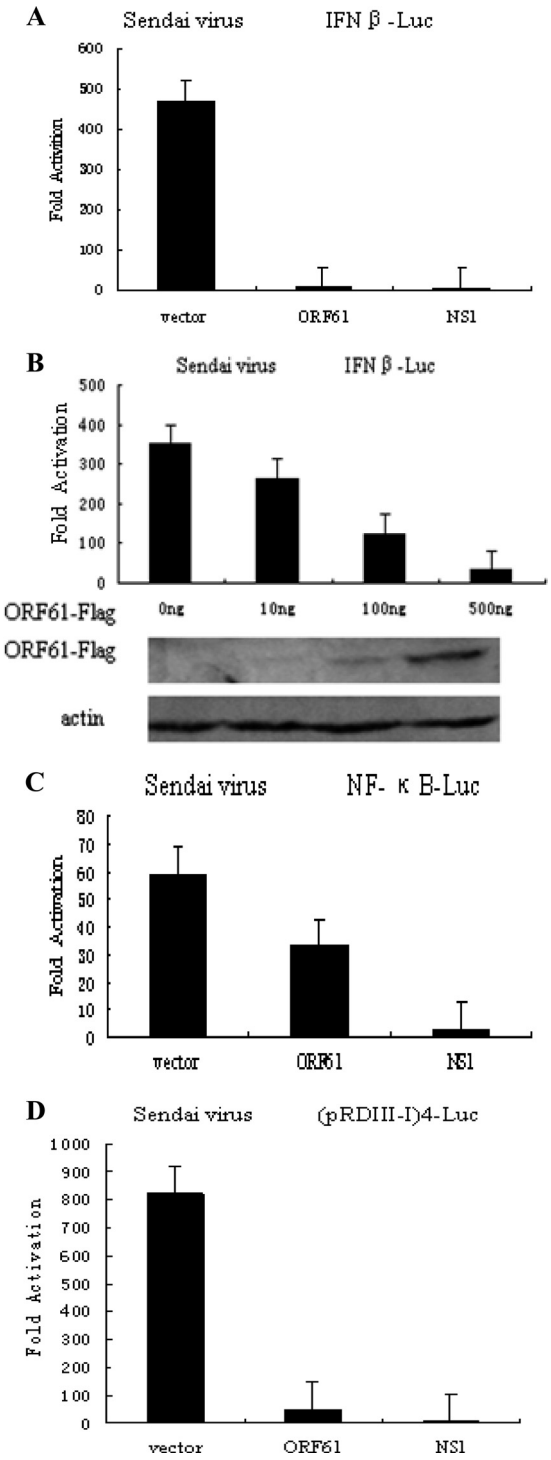

FIG. 2. ORF61 protein inhibits SeV-mediated activation of the IFN-β promoter. HEK 293T cells were cotransfected with IFN-β reporter plasmid p125-luc (A), NF-κB-luc (C), or (pRDIII-I)4-Luc (D) and with the *Renilla* luciferase plasmid pRL-TK and pCMV-Flag empty vector or with plasmids encoding the indicated viral proteins. Twenty-four hours after transfection, cells were infected with 100 HAU/ml SeV or left uninfected, as indicated, and luciferase activity was measured 16 hpi. (B) ORF61-Flag inhibits IFN-β promoter activity in a dose-dependent manner. Data are means and standard deviations from three independent experiments performed in duplicate.

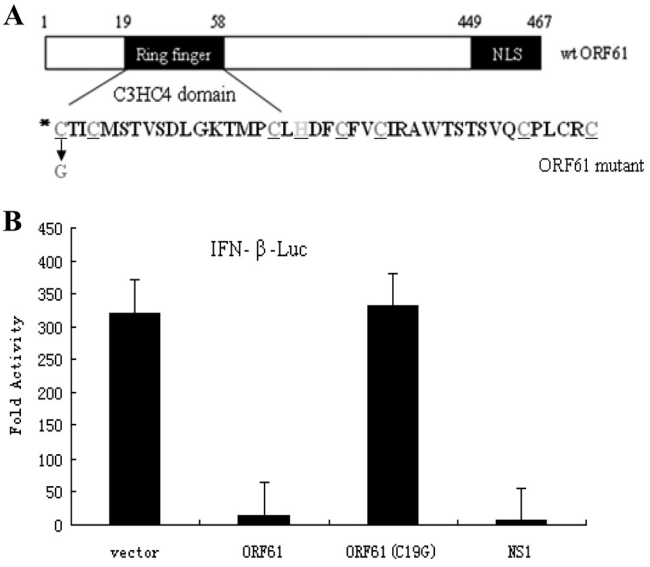

FIG. 3. The inhibition of IFN-β promoter activity by ORF61 is RING finger dependent. (A) Schematic representation of wild type and RING finger mutant (C19G) of ORF61; (B) activation of the IFN-β promoter following SeV infection, measured by DLR assays in the presence of wild-type or mutant ORF61. Data are means and standard deviations from three independent experiments performed in duplicate.

is activated, and type I IFNs can limit VZV replication severely (4, 9, 32), while IFN-β production is not detected in response to poly(I · C) stimulation in VZV-infected human embryonic lung fibroblasts (HELF) (40). During VZV early infection, ORF61 and ORF62 appeared within 1 h (37), which implies that they might play important roles in evasion of innate immunity. To determine the ability of ORF61 to inhibit SeV-mediated activation of IFN-β gene transcription, a Flag-tagged ORF61-expressing plasmid was cotransfected into HEK 293T cells with an IFN-β promoter construct, and the ability of ORF61 to inhibit IFN-β reporter gene activity was examined. SeV infection induced strong IFN-β reporter activity (Fig. 2A). In contrast, ectopic expression of ORF61 or NS1 almost entirely inhibited SeV-mediated activation of IFN-β promoter activity, and the inhibition effect was approximately 50-fold relative to vector (Fig. 2A). Additionally, ORF61 inhibited the IFN-β promoter activity in a dose-dependent manner (Fig. 2B).

The activation of IFN-β gene transcription depends on synergistic interactions among NF-κB, IRFs, and other transcription factors that bind to distinct regulatory domains in the promoter. To examine the role of ORF61 in inhibition of SeV-mediated activation of IRFs and NF-κB, we measured the expression of luciferase reporter genes driven by tandem IRF binding sites in the IFN-β promoter [(pRDIII-I)4-Luc] or NF-κB elements (NF-κB-Luc). SeV infection resulted in strong induction of both NF-κB-Luc and (pRDIII-I)4-Luc reporter activities (Fig. 2C and D). Activation of (pRDIII-I)4 reporter gene construct, which depends on the function of IRFs, was significantly reduced in the presence of ORF61 (Fig. 2D). In contrast, coexpression of ORF61 only slightly affected NF-κB-Luc activity (Fig. 2C). Taken together, these results

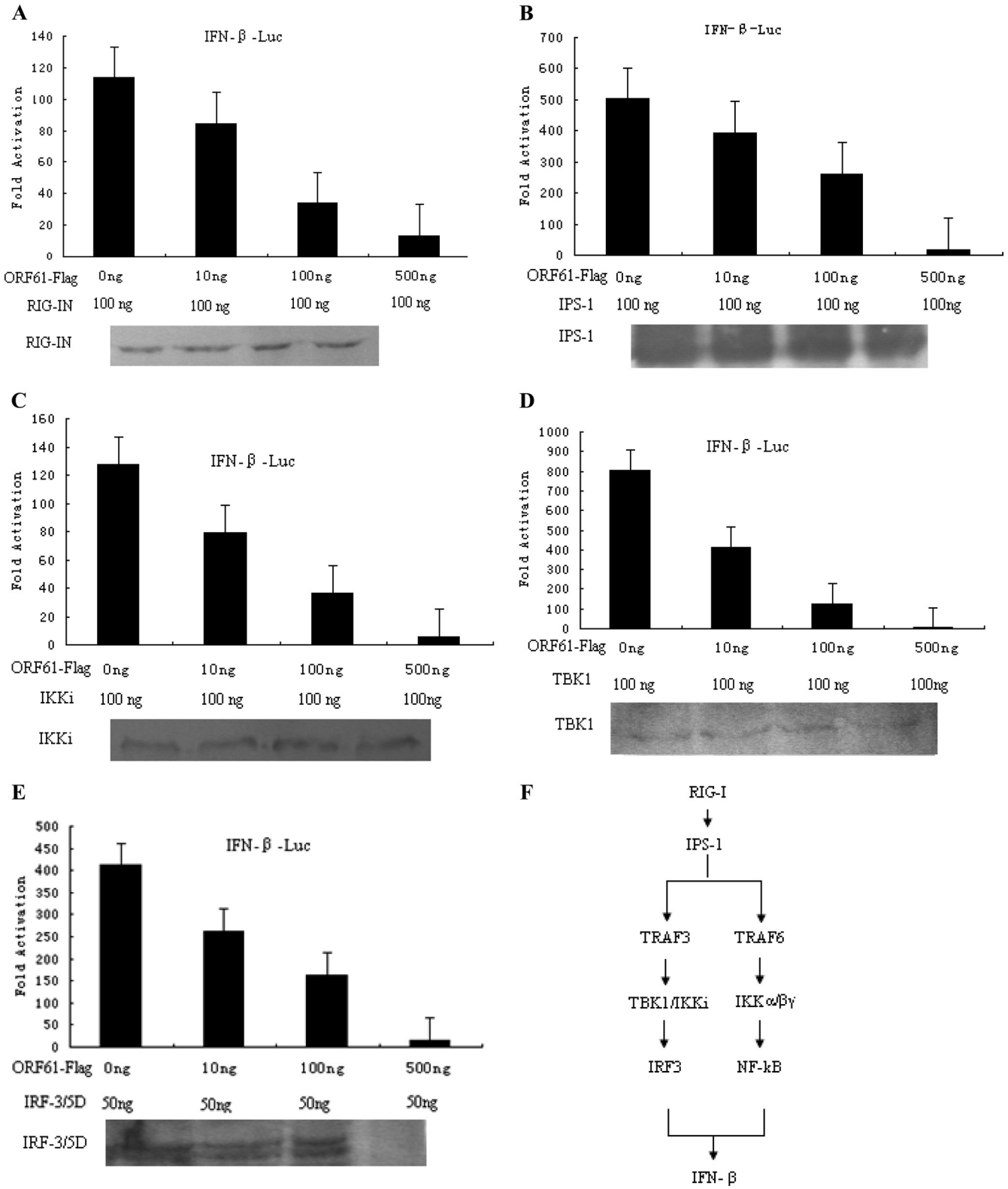

FIG. 4. ORF61 protein inhibits IFN-β promoter activity at the level of IRF3. HEK 293T cells were cotransfected with RIG-IN (A), IPS-1 (B), TBK1 (C), IKKi (D), or IRF3/5D (E) and with the IFN-β reporter plasmid p125-luc and the *Renilla* luciferase reporter plasmid pRL-TK. Thirty-six hours after transfection, luciferase assays were performed. Data are means and standard deviations from three independent experiments performed in duplicate. (F) The IFN-β pathway. The caspase recruitment domains (CARDs) of RIG-I recruit the signaling adaptor protein IFN-β promoter stimulator 1 (IPS-1) after the binding of double-stranded RNA to the helicase domain. IPS-1 resides at the outer mitochondrial membrane and interacts with RIG-I through its CARD. This interaction results in the activity of the TRAF3 and TRAF6 complexes, which leads to the activation of IRF3 and NF-κB, respectively.

demonstrate that ORF61 specifically targets IRFs activation but not the NF-κB pathway.

The inhibition of SeV-mediated activation of IFN-β promoter activity by ORF61 is RING finger dependent. ORF61 bears a C3H4 zinc RING finger domain in the N terminus (Fig. 3A). The RING finger domain is conservative among alphaherpesviruses, and the role of ICP0 in suppressing the host innate immunity is RING finger dependent (23). To determine whether the RING finger domain is also responsible for the ability of ORF61 to inhibit SeV-mediated induction of IFN-β promoter activity, a RING finger mutant of ORF61 was generated by mutation of Cys-19 to Gly (Fig. 3A), a mutation which has been shown to disrupt the RING finger domain (49). The wild-type (wt) ORF61 inhibited SeV-mediated induction of the IFN-β promoter more than 10-fold. However, the C19G mutation of the RING finger domain abrogated the inhibition effect of ORF61 (Fig. 3B), suggesting that the RING finger is critical for the inhibition activity of wt ORF61.

ORF61 inhibits IRF3-mediated transactivation. To further investigate the level at which ORF61 inhibited IFN-β promoter activation, a dose-response curve was performed with increasing amounts of ORF61 and RIG-IN, IPS-1, IKKi, TBK1, and IRF3/5D expression plasmids (Fig. 4). RIG-IN (100 ng) resulted in 100-fold induction of the IFN-β promoter, whereas ORF61 significantly inhibited RIG-IN-mediated activation in a dose-dependent manner (Fig. 4A). When IPS-1, IKKi, TBK1, or IRF3/5D signaling components or transcription factors were applied to activate IFN-β promoter activity (500-, 120-, 800-, and 400-fold, respectively), ORF61 markedly inhibited IPS-1-, IKKi-, TBK1-, or IRF3/5D-mediated IFN-β promoter activity in an essentially similar manner (Fig. 4B to E). The IFN-β pathway is shown in Fig. 4F.

IRF3/5D was also used to activate the ISRE promoter and assess the inhibition activity mediated by ORF61. Similar results were obtained, demonstrating the direct effect of ORF61 on IRF3-mediated transactivation (Fig. 5A). In contrast, ORF61 had no effect on the activity of the ISRE promoter activated by IRF7(6D) (Fig. 5B). Collectively, these results demonstrated that ORF61 inhibited IFN-β promoter activity at the level of IRF3.

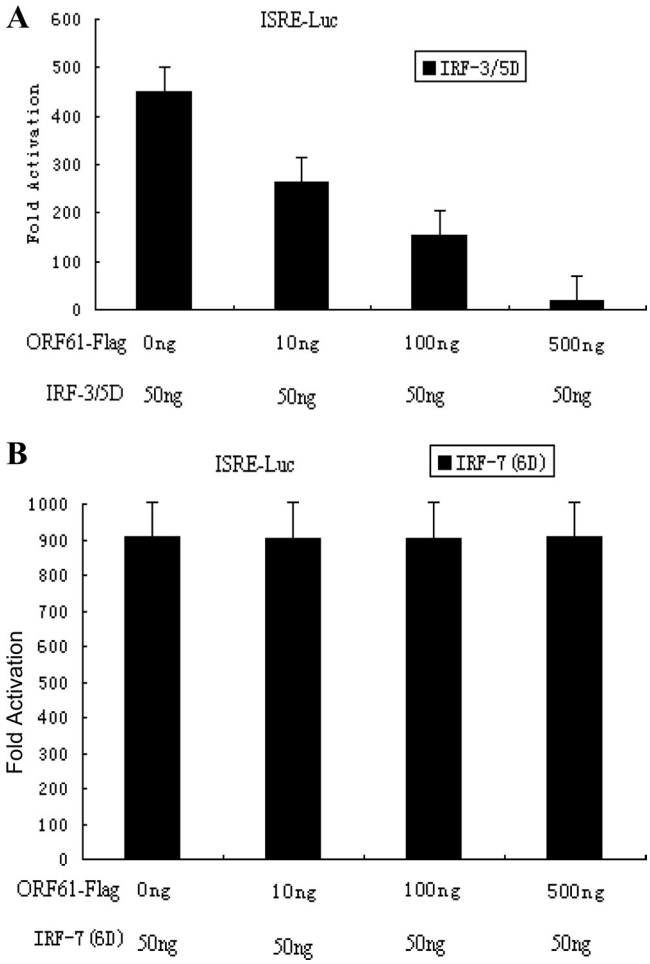

FIG. 5. ORF61 protein suppresses the ISRE promoter activity activated by IRF3 but not IRF7. HEK 293T cells were cotransfected with IRF3/5D (A) or IRF7(6D) (B) and with the ISRE reporter plasmid ISRE-luc and the *Renilla* luciferase reporter plasmid pRL-TK. At 36 h after transfection, DLR luciferase assays were performed. Data are means and standard deviations from three independent experiments performed in duplicate.

ORF61 targets activated IRF3 for proteasome-mediated degradation. Dormant IRF3 is activated by C-terminal phosphorylation, which promotes dimerization, cytoplasm-to-nucleus translocation, DNA binding, association with CBP/p300 histone acetyltransferases and transactivation of downstream target genes (53). The data presented above prompted us to dissect the molecular mechanism of the attenuation effect of ORF61 on IRF3. HeLa cells were transiently transfected with ORF61 or ORF61(C19G) or left untransfected; 24 h later, the cells were infected with SeV or left uninfected, and an immunofluorescence assay was performed at 8 hpi to detect the nuclear translocation of endogenous IRF3. In noninfected cells, IRF3 localized exclusively to the cytoplasm, and ORF61 did not affect the expression or subcellular localization of IRF3 (Fig. 6A). Interestingly, in SeV-infected cells, endogenous IRF3 could not be detected in either the cytoplasm or the nucleus in the presence of ORF61, whereas in the absence of ORF61, IRF3 translocated to the nucleus (Fig. 6B). Strikingly, ORF61(C19G) does not affect the subcellular localization of IRF3 in SeV-stimulated cells (Fig. 6D). It has been demonstrated that virus-dependent phosphorylation of IRF3 constitutes a signal for subsequent proteasome-mediated degradation (53). To determine whether the expression of ORF61 promoted proteasome-mediated degradation of IRF3, SeV-infected cells were treated with the proteasome inhibitor MG132. As shown in Fig. 6C, the treatment of MG132 blocked virus-induced IRF3 degradation, and IRF3 was detected in the nucleus (Fig. 6C). These results indicated that ORF61 targets the active form of IRF3 for degradation. Ser-396 is targeted *in vivo* for phosphorylation following virus infection and plays an essential role in IRF3 activation (42). Therefore, the phosphorylation state of IRF3 following SeV infection was evaluated by immunoblotting using the phospho-specific IRF3(S396) antibody. SeV induced the accumulation of Ser-396 phosphorylation (Fig. 7A, lane 2), and SeV-induced Ser-396 phosphorylation was almost completely blocked by ORF61 (Fig. 7A, lane 4). In contrast, treatment of the cells with MG132 abrogated the degradation of phosphorylated IRF3 (Fig. 7A, lane 5). Furthermore, ORF61(C19G) could not promote degradation of

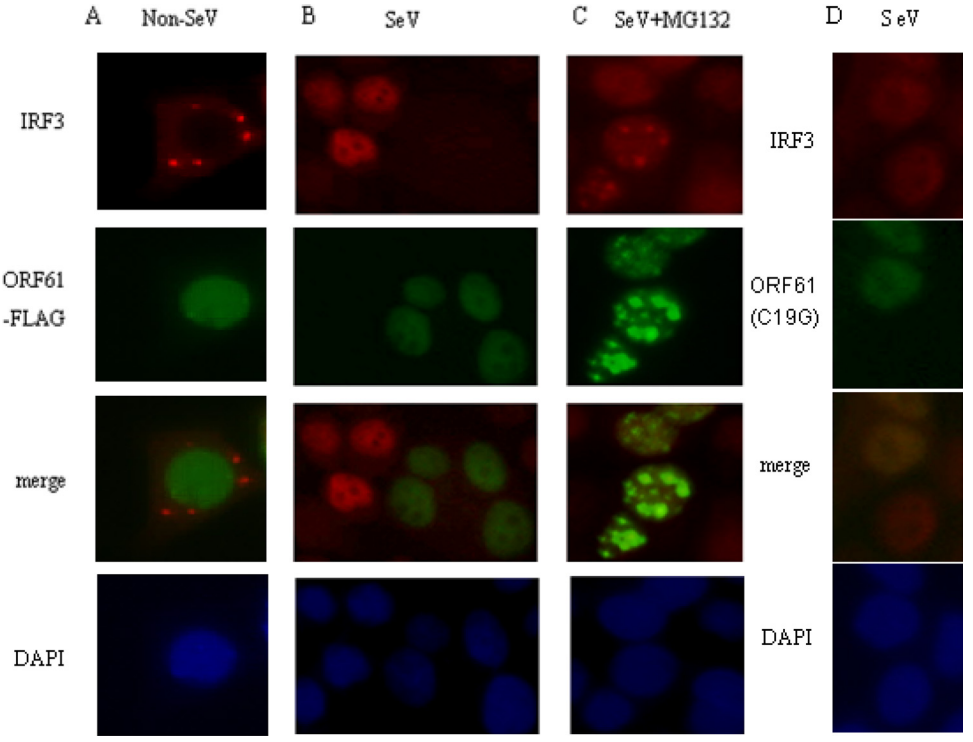

FIG. 6. ORF61 protein targets activated IRF3 for degradation. HeLa cells were cotransfected with the ORF61-Flag (A, B, and C) or the ORF61 RING finger mutant (D) expression plasmid; 24 h after transfection, cells were infected with 100 HAU/ml SeV (B, C, and D) or left uninfected (A), and the proteasomal inhibitor MG132 (10 μM) was added (C) at 1 hpi and maintained in the medium until fixation at 8 hpi. The cells were stained with rabbit anti-IRF3 PAb.

phosphorylated IRF3(S396) (Fig. 7A, lane 6 and lane 7), which confirmed that Cys-19 is a critical amino acid for the RING finger domain of ORF61.

Protein degradation is mostly mediated by the ubiquitin-proteasome system, and E3 ligase usually determines substrate specificity; therefore, as an E3 ubiquitin-protein ligase bearing a typical Cys3-His-Cys4 RING finger domain, ORF61 may mediate the ubiquitination of activated IRF3, according to the results shown in Fig. 7A. Therefore, we tested whether the endogenous activated IRF3 stimulated by SeV underwent ubiquitination in the presence of ORF61. HEK 293T cells were cotransfected with a ubiquitin-HA plasmid and an ORF61-Flag plasmid or left untransfected (Fig. 7B) or were cotransfected with ubiquitin-HA plasmid and ORF61(C19G) or left untransfected (Fig. 7C). Twenty-four hours later, cells were infected with SeV or left uninfected (Fig. 7B and C); cells were also treated with MG132 or left untreated (Fig. 7B and C). After 16 h, cells were collected with lysis buffer, and samples were subjected to WB analysis. Interestingly, when MG132 treatment was used, activated IRF3 in SeV-infected cells was ubiquitinated in the presence of ORF61 and ubiquitin (Fig. 7B, lane 5), while without MG132 treatment, ubiquitinated IRF3 could not be detected (Fig. 7B, lane 4). In addition, ORF61(C19G) failed to promote ubiquitination of IRF3 in any condition. These results demonstrated that only activated IRF3 could be ubiquitinated in the presence of ORF61 with an intact RING finger domain.

Taken together, these results demonstrated that ORF61 specifically promotes phosphorylated IRF3 for proteasome-mediated degradation.

ORF61 mediates the degradation of activated IRF3 via direct interaction. According to the results in Fig. 6C, ORF61 colocalized partly with IRF3 in the nucleus, which led us to further investigate whether ORF61 interacted with phosphorylated IRF3. HEK 293T cells were cotransfected with ORF61-EYFP and IRF3-Flag plasmids; 24 h later, cells were infected with SeV and treated with MG132 at the same time. After 16 h, cells were collected and subjected to a co-IP assay. ORF61 interacted with IRF3 *in vivo* (Fig. 8A). Co-IP assay was also performed to further determine whether ORF61 specifically interacted with phosphorylated IRF3 or unphosphorylated IRF3. ORF61 interacted with phosphorylated IRF3 (with SeV infection) (Fig. 8B) but not unphosphorylated IRF3 (without SeV infection) (Fig. 8C). The results suggested that ORF61 targets only phosphorylated IRF3 for degradation by direct interaction.

ORF61 downregulates the mRNA level of ISGs downstream of IFN-β signaling pathway. To determine the effect of ORF61 on downstream IFN signaling, a semiquantitative RT-PCR assay was performed to measure the mRNA level of ISG54 and ISG56 (Fig. 9). As a result, ORF61 significantly reduced the levels of ISG54 and ISG56 mRNAs (Fig. 9, lane 3), while the treatment of MG132 abrogated the inhibition function of ORF61 (Fig. 9, lane 2), which correlated with the results above. These results demonstrated that ORF61 represses the

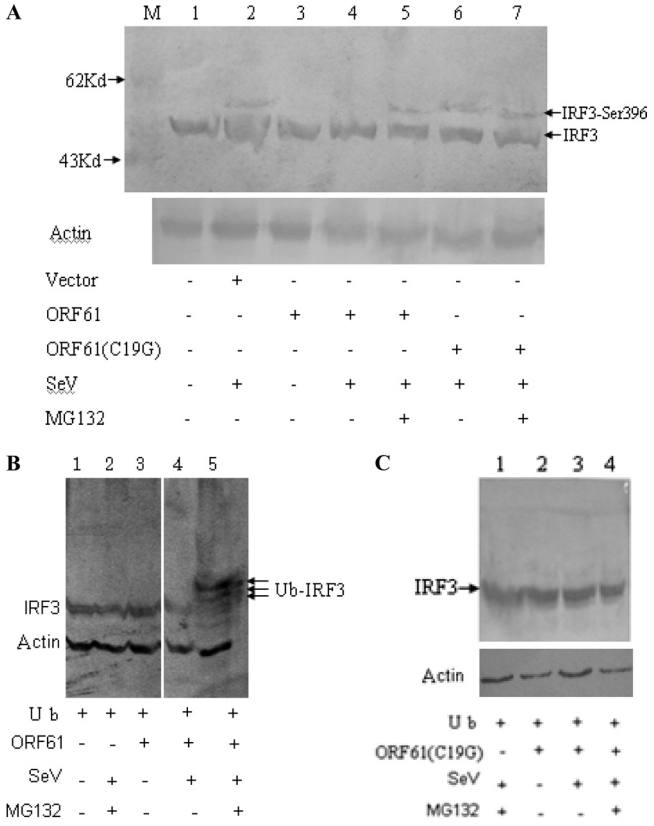

FIG. 7. ORF61 targets phosphorylated IRF3 for proteasome-mediated degradation. (A) HEK 293T cells were transfected with ORF61-Flag (lanes 3, 4, and 5) or ORF61(C19G) (lanes 6 and 7) plasmids or with vector (lane 2) or left untransfected (lane 1). Twenty-four hours after transfection, cells were infected with SeV or left uninfected, and the proteasomal inhibitor MG132 (10 μM) was added (lanes 5 and 7) at 1 hpi and maintained in the medium for 8 h. Whole-cell lysates were separated by SDS-PAGE and detected with phospho-specific antibodies against IRF3(S396). Whole IRF3 was detected together with phosphorylated IRF3 by WB analysis in the same membrane. Actin was detected as a loading control. (B) HEK 293T cells were cotransfected with an HA-ubiquitin expression plasmid and an ORF61-Flag expression plasmid (lanes 3, 4, and 5) or left untransfected (lanes 1 and 2). Twenty-four hours after transfection, cells were infected with SeV (lanes 2, 4, and 5) or left uninfected (lanes 1 and 3), and the proteasomal inhibitor MG132 (10 μM) was added (lanes 2 and 5) at 1 hpi and maintained in the medium for 8 h. Then, whole-cell extracts were collected for Western blot analysis of endogenous IRF3. Actin was detected as a loading control. (C) HEK 293T cells were cotransfected with an HA-ubiquitin expression plasmid and an ORF61(C19G) plasmid (lanes 2, 3, and 4) or left untransfected (lane 1). The assay was performed as described for panel B, and actin was detected as a loading control.

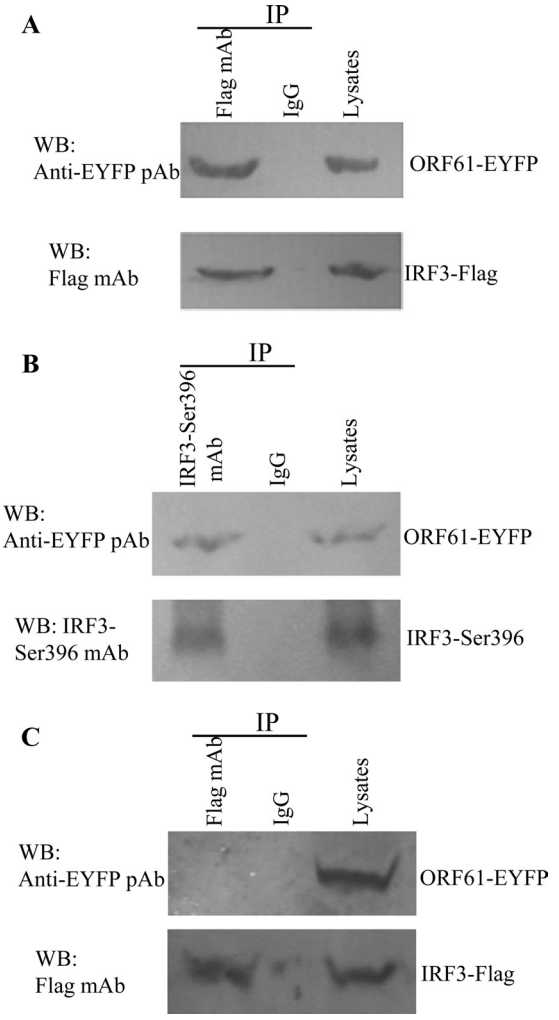

FIG. 8. ORF61 degrades activated IRF3 via direct interaction. (A) HEK 293T cells were cotransfected with ORF61-EYFP and IRF3-Flag plasmids 24 h prior to SeV infection. At the same time, the proteasome inhibitor MG132 (50 μM) was added to medium. At 16 hpi, cells were lysed and subjected to a co-IP assay. Co-IP was also performed with nonspecific antibody (IgG). (B) An ORF61-EYFP plasmid was transfected into HEK 293T cells 24 h prior to SeV infection; MG132 treatment was performed and the co-IP assay was performed as described for panel A. (C) HEK 293T cells were cotransfected with ORF61-EYFP and IRF3-Flag plasmids without SeV infection. The co-IP assay was performed as described for panel A.

IFN downstream signaling pathway via its effect on IRF3 function.

DISCUSSION

Innate immunity is the first line of defense that protects hosts from attacks by pathogenic microbes, and a critical component of this host response is the type I IFN system, including the induction of type I IFNs (α/β IFN), IFN-mediated signaling, and amplification of IFN response. This provides the host with an immediate countermeasure during acute infection to limit initial viral replication and to facilitate an appropriate adaptive immune response (30, 38). In the IFN-β pathway, although the starting point may be different due to various pattern recognition receptors, all signals ultimately converge at IRF3 or IRF7 (8). As reported previously, many viruses can evade host innate immunity at the level of IRF3 and subvert the IFN-β pathway (15, 23). However, little is known about how VZV escapes innate immunity. Results obtained with another alphaherpesvirus, HSV-1, may yield some clues (34). The mechanisms involved in HSV-1 evasion of the host antiviral response have been well elucidated, especially the strategy used by the multifunctional regulated protein ICP0 (6, 18, 23, 26, 43, 46, 54). The function of ICP0 is mostly RING finger

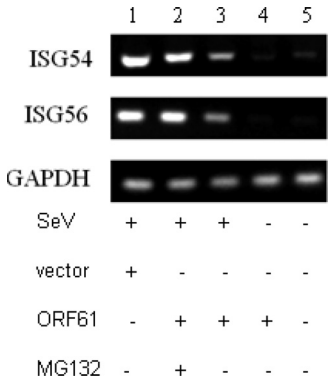

FIG. 9. ORF61 downregulates mRNA of IFN-β and its downstream ISGs. HEK 293T cells were transfected with ORF61-Flag plasmid (lanes 2, 3, and 4); 24 h after transfection, cells were infected with 100 HAU/ml SeV or left uninfected, and the proteasomal inhibitor MG132 (10 μM) was added (lane 2) at 1 hpi and maintained in the medium for 8 h. Semiquantitative RT-PCR analysis was then performed.

dependent, and the ORF61 protein from VZV is homologous to ICP0, indicating that ORF61 may function similarly to ICP0 in many respects, including antagonizing innate immunity.

The question of whether IFN-β is involved in the host defense of VZV infection an important, because IFN-β is one of the most important cytokines in innate immunity, and its role during VZV infection is not well characterized. According to the literature, IFN-α but not IFN-β has been detected in serum during the early phase of VZV infection (20, 40). This raises the question of whether IFN-β was not induced during VZV infection or whether VZV has evolved strategies to block the production of IFN-β. Recently, it was demonstrated that the VZV protein IE62 could block TBK1-mediated IFN-β secretion by targeting IRF3 activation (40); that study was the first report to demonstrate the importance of VZV protein in the control of IFN-β production and uncover a new mechanism among herpesviruses for blocking IRF3 phosphorylation at key serine residues. Another recent publication demonstrated that a highly conserved kinase among herpesviruses named ORF47 could physically interact with IRF3 and induce atypical phosphorylation of IRF3 during VZV infection (48). Interestingly, both publications revealed the important role of VZV proteins in antagonism of the IFN-β pathway at the level of IRF3. IE62 and ORF61 were detected in VZV-infected cells 1 hpi, suggesting that ORF61 might also play an important role in VZV early infection. As we know, in the IFN-β production signal pathway, all signals ultimately converge at IRF3 or IRF7; if a virus has not evolved mechanisms to evade the pathway upstream of IRF3, it may make efforts to inhibit the production of IFN-β in the terminal position, especially an IFN-sensitive virus like VZV. Until recently, no VZV proteins were reported to disturb the IFN-β pathway except IE62. IE62 blocks IRF3 phosphorylation at key serine residues, but the blocking may be incomplete, and part of IRF3 may still be functional during VZV infection; therefore, the new role of ORF61 we reveal here could be a supplemental mechanism for VZV, allowing it to thoroughly block the IFN-β pathway at the IRF3 level. That is, ORF61 may cooperate with IE62 to conquer the innate immunity pathway at the point of IRF3.

Our preliminary screening results (data not shown) demonstrated that ORF61 is the most likely candidate VZV protein in the inhibition of SeV-mediated induction of IFN-β promoter activity in reporter assays. Subsequently, we found that ORF61 can inhibit RIG-IN-, TBK1-, IKKi-, IPS-1-, or IRF3/5D-mediated activation of IFN-β promoter activity. We therefore focused on the effect of ORF61 on IRF3 activation. As demonstrated previously, IRF3 plays a critical role in the host innate immune response, and phosphorylation at a cluster of Ser/Thr residues at the C-terminal end of the protein plays an essential role in its dimerization and activation in the nucleus (41, 47). That may be why so many viruses have evolved strategies to disrupt the innate immune response at the level of IRF3. For example, HSV-1 ICP0 is involved in binding to host IRF3 directly and sequestering it in nuclear bodies away from its normal binding sites on host genes (26). E3L from vaccinia virus exerts its anti-IFN effect by inhibiting the phosphorylation of IRF3 (44). NSP1 of rotavirus is an E3 ubiquitin ligase and causes the degradation of IRF3 by the ubiquitin-proteasome pathway (5). The papain-like protease (PLpro) of SARS coronavirus interacts with IRF3 directly and inhibits its dimerization, thus blocking IRF3 activation (10).

As the conserved E3 ubiquitin ligase among alphaherpesviruses (49), ORF61 may degrade the activated IRF3 via the ubiquitin-proteasome pathway, because the ORF61 mutant with a point mutation in the RING finger domain (C19G) did not affect subcellular localization or protein level (data not shown) of activated IRF3, as shown in Fig. 6D. The fact that ORF61 affects only phosphorylated activated IRF3 may be explained by one of two possibilities. One is that ORF61 mainly localizes in the nucleus, which indicates that the right subcellular localization may correlate with its function. Space consistency may be the crucial factor, because only phosphorylated and activated IRF3 could translocate into the nucleus from the cytoplasm and interact with ORF61. The other possibility is the substrate specificity in the ubiquitin system, in which only activated IRF3 can be a target of ORF61-mediated degradation via the ubiquitin-proteasome pathway. A good example is the degradation of IκB in the NF-κB pathway. In resting cells, NF-κB is usually kept inactive by being sequestered by an inhibitory protein, IκB. But exogenous stimulation leads to the rapid phosphorylation of IκB by a kinase complex called IκB kinase (IKK), and then phosphorylated IκB is recruited to a ubiquitin ligase complex, resulting in degradation (25). Furthermore, co-IP results suggested that ORF61 could mediate the degradation of activated IRF3 via direct interaction. However, bICP0, the bovine herpesvirus 1 homologue of ICP0 (HSV-1) and ORF61 (VZV), induced the degradation of dormant IRF3 (39). Although ICP0 was also reported to disturb the IFN-β pathway at the IRF3 level, its mechanism of action remains to be fully elucidated. While HSV-1 expressing ICP0 enhances Sendai virus-mediated degradation of IRF3 in a coinfection model (26a), no degradation of IRF3 or constituents of the IRF3 pathway have been observed in the context of a single HSV-1 infection (23, 33). Furthermore, nuclear ICP0 failed to block IRF3-dependent induction of ISGs mediated by dsRNA (13a). Thus, the precise molecular mechanism of ORF61 for evading the IFN-β pathway may be distinct from that of ICP0 and bICP0.

ORF61 may be one of the elements used by VZV to inter-

rupt the innate immunity, and more work should be done to reveal the comprehensive mechanisms used by VZV to subvert the host immune response. In conclusion, we have demonstrated that ORF61 mediates the degradation of activated IRF3 in the nucleus via a proteasome-dependent pathway. The mechanism of VZV evasion of the early host antiviral response differs subtly from that of other alphaherpesvirus homologues, suggesting that related viruses within a family evolve evasion mechanisms specific to their particular environment.

ACKNOWLEDGMENTS

This work was supported by grants from the Major State Basic Research Development Program of China (973 Program) (2010CB530105 and 2011CB504802), the Start-up Fund of the Hundred Talents Program of the Chinese Academy of Sciences (20071010-141), the National Natural Science Foundation of China (81000736, 81101263), and the Open Research Fund Program of the State Key Laboratory of Virology of China (2011012).

We thank Zheng-li Shi, Takashi Fujita, S. Ludwig, and Yi-Ling Lin for their gifts of plasmids p125-luc, pEF-FlagRIG-IN, (PRDDIII-)4-Luc, and IRF3/5D, respectively.

REFERENCES

1. **Ambagala, A. P., and J. I. Cohen.** 2007. Varicella-Zoster virus IE63, a major viral latency protein, is required to inhibit the alpha interferon-induced antiviral response. J. Virol. **81:**7844–7851.
2. **Arvin, A. M.** 1996. Immune responses to varicella-zoster virus. Infect. Dis. Clin. North Am. **10:**529–570.
3. **Arvin, A. M.** 2001. Varicella-zoster virus: molecular virology and virus-host interactions. Curr. Opin. Microbiol. **4:**442–449.
4. **Balachandra, K., et al.** 1994. Effects of human alpha, beta and gamma interferons on varicella zoster virus in vitro. Southeast Asian J. Trop. Med. Public Health **25:**252–257.
5. **Barro, M., and J. T. Patton.** 2005. Rotavirus nonstructural protein 1 subverts innate immune response by inducing degradation of IFN regulatory factor 3. Proc. Natl. Acad. Sci. U. S. A. **102:**4114–4119.
6. **Cassady, K. A., and M. Gross.** 2002. The herpes simplex virus type 1 U(S)11 protein interacts with protein kinase R in infected cells and requires a 30-amino-acid sequence adjacent to a kinase substrate domain. J. Virol. **76:**2029–2035.
7. **Chang, T. H., C. L. Liao, and Y. L. Lin.** 2006. Flavivirus induces interferon-beta gene expression through a pathway involving RIG-I-dependent IRF3 and PI3K-dependent NF-κB activation. Microbes Infect. **8:**157–171.
8. **Clement, J. F., et al.** 2008. Phosphorylation of IRF3 on Ser 339 generates a hyperactive form of IRF3 through regulation of dimerization and CBP association. J. Virol. **82:**3984–3996.
9. **Desloges, N., M. Rahaus, and M. H. Wolff.** 2005. Role of the protein kinase PKR in the inhibition of varicella-zoster virus replication by beta interferon and gamma interferon. J. Gen. Virol. **86:**1–6.
10. **Devaraj, S. G., et al.** 2007. Regulation of IRF3-dependent innate immunity by the papain-like protease domain of the severe acute respiratory syndrome coronavirus. J. Biol. Chem. **282:**32208–32221.
11. **Ehrhardt, C., et al.** 2004. Rac1 and PAK1 are upstream of IKK-epsilon and TBK-1 in the viral activation of interferon regulatory factor-3. FEBS Lett. **567:**230–238.
12. **Everett, R. D.** 1984. Trans activation of transcription by herpes virus products: requirement for two HSV-1 immediate-early polypeptides for maximum activity. EMBO J. **3:**3135–3141.
13. **Everett, R. D., et al.** 2006. PML contributes to a cellular mechanism of repression of herpes simplex virus type 1 infection that is inactivated by ICP0. J. Virol. **80:**7995–8005.

13a. **Everett, R. D., and A. Orr.** 2009. Herpes simplex virus type 1 regulatory protein ICP0 aids infection in cells with a preinduced interferon response but does not impede interferon-induced gene induction. J. Virol. **83:**4978–4983.

14. **Gelman, I. H., and S. Silverstein.** 1985. Identification of immediate early genes from herpes simplex virus that transactivate the virus thymidine kinase gene. Proc. Natl. Acad. Sci. U. S. A. **82:**5265–5269.
15. **Hartman, A. L., et al.** 2008. Inhibition of IRF3 activation by VP35 is critical for the high level of virulence of Ebola virus. J. Virol. **82:**2699–2704.
16. **Inchauspe, G., S. Nagpal, and J. M. Ostrove.** 1989. Mapping of two varicella-zoster virus-encoded genes that activate the expression of viral early and late genes. Virology **173:**700–709.
17. **Jordan, M., A. Schallhorn, and F. M. Wurm.** 1996. Transfecting mammalian cells: optimization of critical parameters affecting calcium-phosphate precipitate formation. Nucleic Acids Res. **24:**596–601.
18. **Kim, J. C., et al.** 2008. HSV-1 ICP27 suppresses NF-κB activity by stabilizing IκBα. FEBS Lett. **582:**2371–2376.
19. **Kochs, G., A. Garcia-Sastre, and L. Martinez-Sobrido.** 2007. Multiple anti-interferon actions of the influenza A virus NS1 protein. J. Virol. **81:**7011–7021.
20. **Ku, C. C., et al.** 2004. Varicella-zoster virus transfer to skin by T cells and modulation of viral replication by epidermal cell interferon-alpha. J. Exp. Med. **200:**917–925.
21. **Lin, R., C. Heylbroeck, P. M. Pitha, and J. Hiscott.** 1998. Virus-dependent phosphorylation of the IRF3 transcription factor regulates nuclear translocation, transactivation potential, and proteasome-mediated degradation. Mol. Cell. Biol. **18:**2986–2996.
22. **Lin, R., et al.** 2006. Dissociation of a MAVS/IPS-1/VISA/Cardif-IKKε molecular complex from the mitochondrial outer membrane by hepatitis C virus NS3-4A proteolytic cleavage. J. Virol. **80:**6072–6083.
23. **Lin, R., R. S. Noyce, S. E. Collins, R. D. Everett, and K. L. Mossman.** 2004. The herpes simplex virus ICP0 RING finger domain inhibits IRF3- and IRF7-mediated activation of interferon-stimulated genes. J. Virol. **78:**1675–1684.
24. **Lin, R., et al.** 2006. Negative regulation of the retinoic acid-inducible gene I-induced antiviral state by the ubiquitin-editing protein A20. J. Biol. Chem. **281:**2095–2103.
25. **Magnani, M., R. Crinelli, M. Bianchi, and A. Antonelli.** 2000. The ubiquitin-dependent proteolytic system and other potential targets for the modulation of nuclear factor-κB (NF-κB). Curr. Drug Targets **1:**387–399.
26. **Melroe, G. T., L. Silva, P. A. Schaffer, and D. M. Knipe.** 2007. Recruitment of activated IRF3 and CBP/p300 to herpes simplex virus ICP0 nuclear foci: potential role in blocking IFN-beta induction. Virology **360:**305–321.

26a. **Melroe, G. T., N. A. DeLuca, and D. M. Knipe.** 2004. Herpes simplex virus 1 has multiple mechanisms for blocking virus-induced interferon production. J. Virol. **78:**8411–8420.

27. **Mikloska, Z., A. M. Kesson, M. E. Penfold, and A. L. Cunningham.** 1996. Herpes simplex virus protein targets for CD4 and CD8 lymphocyte cytotoxicity in cultured epidermal keratinocytes treated with interferon-gamma. J. Infect. Dis. **173:**7–17.
28. **Moriuchi, H., M. Moriuchi, H. A. Smith, S. E. Straus, and J. I. Cohen.** 1992. Varicella-zoster virus open reading frame 61 protein is functionally homologous to herpes simplex virus type 1 ICP0. J. Virol. **66:**7303–7308.
29. **Mueller, N. H., D. H. Gilden, R. J. Cohrs, R. Mahalingam, and M. A. Nagel.** 2008. Varicella zoster virus infection: clinical features, molecular pathogenesis of disease, and latency. Neurol. Clin. **26:**675–697.
30. **Muller, U., et al.** 1994. Functional role of type I and type II interferons in antiviral defense. Science **264:**1918–1921.
31. **Nagpal, S., and J. M. Ostrove.** 1991. Characterization of a potent varicella-zoster virus-encoded trans-repressor. J. Virol. **65:**5289–5296.
32. **Otani, N., K. Baba, and T. Okuno.** 2009. Interferon-gamma release assay: a simple method for detection of varicella-zoster virus-specific cell-mediated immunity. J. Immunol. Methods **351:**71–74.
33. **Paladino, P., S. E. Collins, and K. L. Mossman.** 2010. Cellular localization of the herpes simplex virus ICP0 protein dictates its ability to block IRF3-mediated innate immune responses. PLoS One **5:**e10428.
34. **Paladino, P., and K. L. Mossman.** 2009. Mechanisms employed by herpes simplex virus 1 to inhibit the interferon response. J. Interferon Cytokine Res. **29:**599–607.
35. **Pan, W., X. Ren, H. Guo, Q. Ding, and A. C. Zheng.** 2010. Expression, purification of herpes simplex virus type 1 UL4 protein, and production and characterization of UL4 polyclonal antibody. J. Virol. Methods **163:**465–469.
36. **Paz, S., et al.** 2009. Ubiquitin-regulated recruitment of IκB kinase epsilon to the MAVS interferon signaling adapter. Mol. Cell. Biol. **29:**3401–3412.
37. **Reichelt, M., J. Brady, and A. M. Arvin.** 2009. The replication cycle of varicella-zoster virus: analysis of the kinetics of viral protein expression, genome synthesis, and virion assembly at the single-cell level. J. Virol. **83:**3904–3918.
38. **Sadler, A. J., and B. R. Williams.** 2008. Interferon-inducible antiviral effectors. Nat. Rev. Immunol. **8:**559–568.
39. **Saira, K., Y. Zhou, and C. Jones.** 2007. The infected cell protein 0 encoded by bovine herpesvirus 1 (bICP0) induces degradation of interferon response factor 3 and, consequently, inhibits beta interferon promoter activity. J. Virol. **81:**3077–3086.
40. **Sen, N., et al.** 2010. Varicella-zoster virus immediate-early protein 62 blocks interferon regulatory factor 3 (IRF3) phosphorylation at key serine residues: a novel mechanism of IRF3 inhibition among herpesviruses. J. Virol. **84:**9240–9253.
41. **Servant, M. J., N. Grandvaux, and J. Hiscott.** 2002. Multiple signaling pathways leading to the activation of interferon regulatory factor 3. Biochem. Pharmacol. **64:**985–992.
42. **Sharma, S., B. R. tenOever, N. Grandvaux, G. P. Zhou, R. Lin, and J. Hiscott.** 2003. Triggering the interferon antiviral response through an IKK-related pathway. Science **300:**1148–1151.
43. **Shibaki, T., T. Suzutani, I. Yoshida, M. Ogasawara, and M. Azuma.** 2001. Participation of type I interferon in the decreased virulence of the UL13 gene-deleted mutant of herpes simplex virus type 1. J. Interferon Cytokine Res. **21:**279–285.
44. **Smith, E. J., I. Marie, A. Prakash, A. Garcia-Sastre, and D. E. Levy.** 2001.

IRF3 and IRF7 phosphorylation in virus-infected cells does not require double-stranded RNA-dependent protein kinase R or Iκ B kinase but is blocked by Vaccinia virus E3L protein. J. Biol. Chem. **276:**8951–8957.
45. **Stevenson, D., K. L. Colman, and A. J. Davison.** 1992. Characterization of the varicella-zoster virus gene 61 protein. J. Gen. Virol. **73**(Pt. 3)**:**521–530.
46. **Suzutani, T., et al.** 2000. The role of the UL41 gene of herpes simplex virus type 1 in evasion of non-specific host defence mechanisms during primary infection. J. Gen. Virol. **81:**1763–1771.
47. **Taniguchi, T., K. Ogasawara, A. Takaoka, and N. Tanaka.** 2001. IRF family of transcription factors as regulators of host defense. Annu. Rev. Immunol. **19:**623–655.
48. **Vandevenne, P., et al.** 2011. The varicella-zoster virus ORF47 kinase interferes with host innate immune response by inhibiting the activation of IRF3. PLoS One **6:**e16870.
49. **Walters, M. S., C. A. Kyratsous, and S. J. Silverstein.** 2010. The RING finger domain of Varicella-Zoster virus ORF61p has E3 ubiquitin ligase activity that is essential for efficient autoubiquitination and dispersion of Sp100-containing nuclear bodies. J. Virol. **84:**6861–6865.
50. **Xing, J., et al.** 2011. Comprehensive characterization of interaction complexes of herpes simplex virus type 1 ICP22, UL3, UL4, and UL20.5. J. Virol. **85:**1881–1886.
51. **Xing, J., F. Wu, W. Pan, and C. Zheng.** 2010. Molecular anatomy of subcellular localization of HSV-1 tegument protein US11 in living cells. Virus Res. **153:**71–81.
52. **Yoneyama, M., et al.** 2004. The RNA helicase RIG-I has an essential function in double-stranded RNA-induced innate antiviral responses. Nat. Immunol. **5:**730–737.
53. **Zhang, B., et al.** 2009. The TAK1-JNK cascade is required for IRF3 function in the innate immune response. Cell Res. **19:**412–428.
54. **Zhang, C., et al.** 2008. A conserved domain of herpes simplex virus ICP34.5 regulates protein phosphatase complex in mammalian cells. FEBS Lett. **582:**171–176.
55. **Zhang, Z., et al.** 2007. Genetic analysis of varicella-zoster virus ORF0 to ORF4 by use of a novel luciferase bacterial artificial chromosome system. J. Virol. **81:**9024–9033.
56. **Zhao, T., et al.** 2007. The NEMO adaptor bridges the nuclear factor-κB and interferon regulatory factor signaling pathways. Nat. Immunol. **8:**592–600.
57. **Zhong, B., et al.** 2008. The adaptor protein MITA links virus-sensing receptors to IRF3 transcription factor activation. Immunity **29:**538–550.
58. **Zhu, H., and Zheng, C.** 2011. Varicella zoster virus immediate early protein 61 blocks the IFN-β pathway by degradation the activited [sic] IRF3. BMC Proc. **5**(Suppl. 1)**:**P99.